Simulation of Lunar Soil Excavation and Landfill in the Lunar Power Station Construction

Yuena He
School of Mechatronics Engineering and Automation
Shanghai University
Shanghai, China
2541580032@shu.edu.cn

Weiyang Xu
Shanghai Institute of Aerospace System Engineering
Shanghai, China
429703329@qq.com

Meng Chen
Shanghai Institute of Aerospace System Engineering
Shanghai, China
workmailcm@126.com

Xiaoyu Wang
School of Mechatronics Engineering and Automation
Shanghai University
Shanghai, China
xiaoyu24725096@shu.edu.cn

Zimeng Gao
School of Mechatronics Engineering and Automation
Shanghai University
Shanghai, China
gaozimeng@shu.edu.cn

Wenwei Qiu
School of Mechatronics Engineering and Automation
Shanghai University
Shanghai, China
qiuwenwei@shu.edu.cn

Hang Shi*
School of Mechatronics Engineering and Automation
Shanghai University
Shanghai, China
hangshi@shu.edu.cn

2025 5th International Symposium on Computer Technology and Information Science (ISCTIS) | 979-8-3315-4450-8/25/$31.00 ©2025 IEEE | DOI: 10.1109/ISCTIS65944.2025.11065032

***Abstract*—This paper presents a lunar soil excavation and backfilling method based on simulation technology, aiming to address the challenges of low-cost operation verification in the construction of lunar surface power station. To handle the complex terrain and non-uniform lunar soil characteristics in the extreme lunar environment, the research adopts finite element mesh subdivision and Mini-Batch K-means clustering algorithm to discretize the area to be excavated into tetrahedral cells and cluster them into excavation blocks to improve the realism in the simulation. By combining the layering strategy with the Zig-zag path planning algorithm, the operation sequence of excavation and landfill is optimized. Finally, the excavation block geometry model is reconstructed and the STL model is exported to provide a high-fidelity dynamic verification platform for Gazebo and ROS co-simulation. The simulation results show that the method has significant advantages in terms of the fidelity lunar soil operations, and provides reliable technical support for the construction of power stations in future lunar exploration missions.**

Keywords—lunar power station; simulation; lunar soil excavation and landfill; Zig-zag path planning

I. INTRODUCTION

As lunar exploration missions continue to progress, the development of surface power stations has become critical infrastructure to support long-term operations on the Moon. Future lunar missions will demand significant advances in power systems[1]. However, existing studies indicate that the cost of delivering power to the lunar surface is as high as $700,000/kg, as is the cost of nighttime energy supply technologies[2]. Therefore, achieving efficient and low-cost energy supply on the lunar surface remains a central challenge in the lunar power station construction.

At present, solar and nuclear power are the most commonly proposed solutions for lunar surface energy generation. However, solar panels are costly, while nuclear fission is capable of generating electricity for long periods of time using a very limited amount of fuel[3]. In 2007 NASA's Lunar Architecture Team proposed a fission surface power (FSP) system architecture[4] that utilizes compact nuclear reactors to supply energy to lunar bases[5]. The most recent advancement in space nuclear power is the US Kilopower project[6]. It involves placing a compact nuclear reactor in a crater approximately two meters deep. This configuration includes a shield to protect surrounding systems from direct radiation exposure[7].

Based on the previous design, this study proposes a configuration in which the reactor core is buried within an excavation pit. Lunar soil serves as a natural radiation shielding material, while non-nuclear components are mounted on a surface-level truss structure. This solution not only addresses the radiation shielding challenges, but also provides better maintainability than conventional reactor configurations. The architecture combines the reliability of fission energy with innovative construction methods adapted to the lunar environment.

Although existing energy solutions provide a foundational framework for supporting lunar research stations[8], the construction of lunar power stations still faces significant technical challenges. These include extreme temperature fluctuations, ultrahigh vacuum conditions, intense radiation exposure, and reduced gravity[9]. However, traditional experimental methods are insufficient for accurately replicating the lunar environment and evaluating system performance under realistic conditions. Therefore, a robust simulation methodology is urgently needed to support the engineering design and validation of lunar surface power stations. To intuitively demonstrate the key tasks in the simulation of lunar surface power station construction, the simulation scenario is shown in Fig. 1. The robot performs lunar soil excavation, as shown in (a). The backfilling process is shown in (b). In the simulation, the robot system performs lunar soil excavation and covering tasks according to the predetermined trajectory, effectively replicating the dynamic process of the actual deployment of the lunar surface power station.

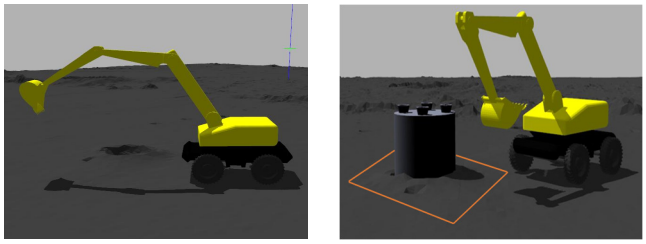

(a) Excavation processes (b) Landfill processes

Fig. 1. Work process

In recent years, with the advancement of virtual physics engines and robotics middleware, several high-fidelity simulation platforms have been developed to accurately simulate the dynamics and kinematics of lunar surface exploration missions. These include Gazebo[10], V-REP[11], and Webots[12] and enable researchers to efficiently simulate lunar surface environments. However, existing studies have primarily focused on the trajectory planning and system-level validation of lunar exploration equipment, such as Planetary Rover Simulation[13] and lunar rover[14]. These investigations include the generation of synthetic imagery for evaluating human-robot interaction in navigation tasks and improving the resolution of lunar digital elevation models[13], as well as high-fidelity simulation systems for lunar rovers that emphasize technologies such as geomechanics and recursive dynamics[14]. In the construction of power stations on the lunar surface, there is a lack of in-depth exploration of the lunar soil excavation and backfilling process. This gap limits the comprehensive modelling and validation of the construction phase of lunar energy systems.

Based on the particularity of the lunar surface environment and the gaps in previous research, this paper proposes a lunar soil excavation and landfill plan for the construction of a lunar power station. The focus is on simulating the process of operating a robot to excavate and backfill the excavated area. It includes finite-element discretization of the material to be removed, a Mini-Batch K-means clustering algorithm[15] to fit a single excavation job. It reduces the amount of computation and memory consumption of the iteration, and at the same time ensures high clustering accuracy[16]. A three-dimensional coverage area planning algorithm is used to achieve full area excavation planning. After the cores are placed at the designated location in the pit, the robot fills the cores in the planned filling sequence. Section II describes in detail the discretization and clustering of the whole area to be excavated and landfilled, the path planning of the excavated and landfilled blocks and the whole process of model export. Section III shows the complete simulation process of the proposed method in Gazebo combined with ROS to verify the feasibility of the method in practical applications.

II. METHODOLOGY

In this study, a simulation method for excavation and landfill in the construction of a lunar surface power station is proposed. It combines finite element mesh discretization, Mini-Batch K-means clustering analysis, Zig-zag path planning and STL model export and the whole process is shown in Fig. 2. In this section, the specific implementation steps of the method are described in detail, including discretization and clustering of excavation areas, path planning, STL export and dynamic visualization.

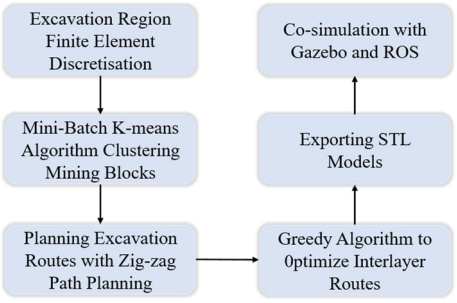

Fig. 2. Flowchart of the method

A. Excavation Area Discretisation and Clustering Modelling

1) Area Modelling and Mesh Discretisation

Taking the excavation area in Fig. 1 is used as an example of this part of the area. To ensure the realism of the simulation, this paper first selects appropriate lunar craters based on the virtual prediction results of the lunar surface, and divides the excavation area into the area to be excavated S_{work}, and the area to be filled S_{fill}, as shown in Fig. 3 .

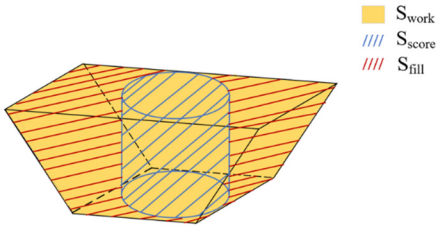

Fig. 3. Schematic diagram of the area of operation

Next, the area to be excavated is tetrahedrally discretised using the finite element method (FEM) to form a mesh surface formed by multiple triangular facets as shown in Fig. 4. The purpose of meshing is to transform a complex 3D space into an easily solvable discrete model through nodes and elements. To ensure the fineness of the mesh, tetrahedral mesh cells are used in this study, which can well simulate the shape of the moon crater. The maximum cell length is set to be 0.05, and the shortest edge length is not less than 0.025. In this study, quadratic grid cells are used . Discrete node and element data are finally generated.

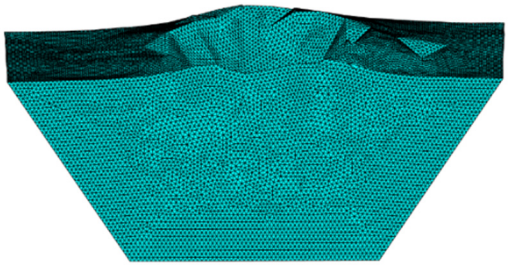

Fig. 4. Schematic of discrete areas to be excavated

2) Tetrahedral Clustering

The clustering process involves clustering the discretized micro-tetrahedron into reasonable single excavation blocks

based on the volume capacity of one excavation. In this study, the geometrical significance of the mixed product is exploited to compute the volume V and the center of mass coordinates of the space tetrahedron from the coordinates of the four vertices A $\left(x_1,y_1,z_1\right)$, B $\left(x_2,y_2,z_2\right)$, C $\left(x_3,y_3,z_3\right)$, D $\left(x_4,y_4,z_4\right)$.

$$V=\frac{1}{6}\left|\left(\overrightarrow{BA}\times\overrightarrow{CA}\right)\bullet\overrightarrow{DA}\right|=\frac{1}{6}\det\begin{pmatrix}1&1&1&1\\x_1&x_2&x_3&x_4\\y_1&y_2&y_3&y_4\\z_1&z_2&z_3&z_4\end{pmatrix} \quad (1)$$

$$G=\left(\frac{x_1+x_2+x_3+x_4}{4},\frac{y_1+y_2+y_3+y_4}{4},\frac{z_1+z_2+z_3+z_4}{4}\right) \quad (2)$$

The volume of multiple tetrahedrons after discretization is calculated according to (1). The centroid coordinates are obtained according to (2). Based on these data, the center of mass is clustered using a Mini-Batch K-Means clustering algorithm.

Mini-Batch K-Means updates the cluster centers by using only a small random subset of the dataset at a time, where m is the number of data points belonging to cluster i in the current batch; b_i is the set of data points belonging to cluster i in the current batch; c_i is the current center position of cluster i; and n_i is the total number of data points assigned to cluster i so far. The update formula is shown in (3).

$$c_i:=\left(1-\frac{m}{n_i-m}\right)c_i+\frac{m}{n_i-m}\overline{b}_i \quad (3)$$

Compared with the traditional K-means algorithm, the Mini-Batch K-means clustering algorithm selects only a small portion of samples in the dataset for updating each time. By this method, the tetrahedra to be mined are clustered into multiple 'excavation blocks', which provides the basis for path planning and job execution. Fig. 5 exhibits the clustering blocks along with their volume ranges.

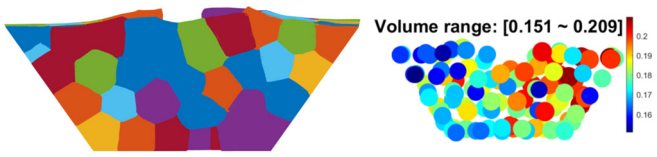

Fig. 5. Schematic representation of the clustering blocks and their volumes in the area to be mined

B. Route Planning for Digging Shovels

Different from the traditional planar coverage path planning, excavation operations have obvious volume and hierarchical characteristics, and must follow the top-to-bottom, layer-by-layer advancement of the operating sequence to avoid structural interference and material obstruction. The use of hierarchical path planning in the excavation area helps to simplify the complex three-dimensional operation task into a number of easy-to-handle two-dimensional coverage problems, which improves the controllability of the path generation, and effectively reduces the energy consumption and execution complexity caused by path jumping. Previous studies have proposed complex 3D coverage path planning in underwater environments[17]. The method is also applicable in the lunar surface environment. The excavation operation requires a hierarchical path planning strategy for this study, combined with the Zig-zag path planning algorithm, to efficiently cover the clustering blocks in the excavation to-be-excavated region. In the layered strategy, the excavation blocks are layered according to the height corresponding to the volume, and if the center of mass of an excavation block is higher than the range of a certain layer, it is considered that the block belongs to this layer. Using the centroid coordinates of the clustering blocks and dividing all blocks into several layers according to the Z-axis direction, the height of each layer is obtained, as shown in (4).

$$h=\frac{z_{\max}-z_{\min}}{N} \quad (4)$$

The layer number to which the excavated block belongs is calculated, as shown in (5). In this study, downward rounding is used. The layering effect is shown in Fig. 6.

$$L_i=\min\left(\left\lfloor\frac{z_i-z_{\min}}{h}\right\rfloor+1,N\right) \quad (5)$$

Fig. 6. Layering of excavation block

After completing the layering, Zig-zag path planning is applied to each layer. Zig-zag path planning simplifies complex 2D maps with irregular shapes[18], enabling path computation. Therefore, in this study, the excavation blocks in the region are grouped according to the y-axis and the grouping threshold $\triangle y$ is set according to the volume range of each block. For the *ith* excavation block G_i, if $\left|y_i-y_{current}\right|<\triangle y$,then it is added to the current group, otherwise a new group is opened, there are shown in (6).

$$G_i=\left\{B_i\left|y_i-y_{current}\right|<\triangle y\right\} \quad (6)$$

After the grouping in the Y-axis direction is completed, ascending ordering is performed in the X-axis, and the paths in the odd-even array are reversed to form a Z-shaped arrangement. The interlayer path planning for each layer is shown in Fig. 7.

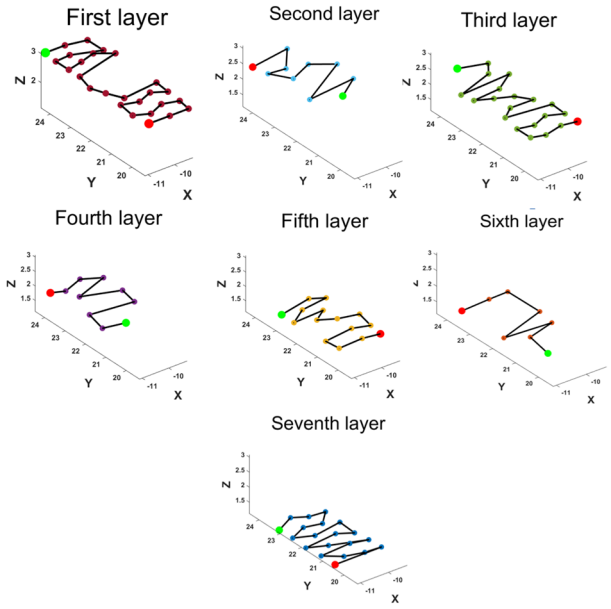

Fig. 7. Intra-layer excavation route planning results

A strategy based on the Greedy algorithm is introduced in the inter-layer connection process of path planning. Specifically, at the end of each layer, the block with the closest distance is selected as the starting point of the next layer by calculating the Euclidean distance between the last block of the current layer and all the blocks of the next layer. Subsequently, the path order of the next layer is dynamically adjusted so that the path starts from that nearest block and is reordered according to the reverse traversal. This approach not only reduces the distance between layer jumps, but also improves the overall continuity of the path. The overall planning path is shown in Fig. 8.

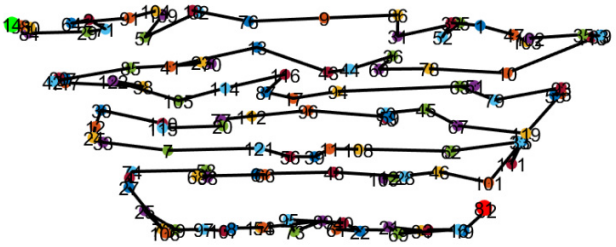

Fig. 8. Overall excavation route planning results

The path lengths between layers are exhibited in TABLE 1.

Table 1 The length of the path between layers.

From Layer	***To Layer***	***Length***
1	2	1.82
2	3	1.11
3	4	0.78
4	5	1.23
5	6	0.52
6	7	0.71

C. Excavation Block Export

To realize the simulation effect in real construction, the geometry of each excavation block needs to be reconstructed. The node coordinates and cell topology relationships of the identified blocks and their corresponding block indexes are used as inputs to process the data of each block one by one. The unit number of its corresponding block is extracted from the global set of units, and the Alpha shape algorithm[19] extracts the boundary envelope of the nodes of each block, which is exported as an STL model.

III. SIMULATION AND DISCUSSION

A. Quality and Efficiency of Clustering

When digging the region for discretization, different Target maximum mesh edge lengths are chosen to get different Mesh nodes, Mesh elements, number of mesh contained in the maximum clustering block, program running time, and average volume of clustering blocks. In TABLE 2 , *Hmax* indicates the Target maximum mesh edge length, *Number* indicates the number of mesh contained in the maximum clustering block, *Time* indicates the time needed for discretization and clustering, and *Volume* indicates the average volume of the clustering block.

Table 2 Discrete data with different precision

Hmax	*Number*	*Elements*	*Nodes*	*Time*	*Volume*
0.035	43531	4311156	5812042	304.29	0.1794
0.037	37638	3650503	4926705	197.34	0.1792
0.04	32743	2883403	3897214	139.09	0.1795
0.05	13966	1475025	2004260	80.19	0.1805
0.1	2037	175339	246713	10.78	0.1813
0.5	37	1891	3336	2.18	0.1786
1	16	643	1232	2.04	0.1824
1.5	13	259	563	2.02	0.1776
3	7	183	402	2.01	0.1748
9	5	129	290	2.02	0.1706
10	4	128	288	2.01	0.1706

During the clustering process, volume constraints are imposed on the clustering blocks because of the limitations of the excavation shovel capacity. Clustering blocks range in volume from 0.15 to 0.21 cubic meters with a target volume of 0.18 cubic meters. The effectiveness of the clustering is assessed by calculating the absolute value of the absolute error between the average volume of the clustering blocks and the target volume, and determining whether the block volume is as expected. If the error is large, it means that the clustering effect is not good. From Fig. 9 , it can be seen that as *Hmax* increases, the program running time decreases while the error increases. Therefore in this study, *Hmax* is set to 0.05, as marked in Fig. 9.

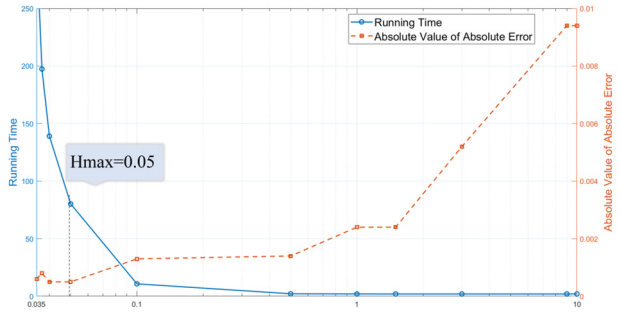

Fig. 9. Error and runtime curves

B. *Disaggregation and Clustering of Landfill Areas*

Perform the same segmentation, clustering and path planning for the landfill area after removing the core. Modify the number of layers according to the actual condition of the landfill area. It is finally clustered into 87 valid landfill blocks. In planning the excavation path, the landfill blocks are firstly divided into 4 layers and then the route is planned between the layers using the Zig-zag algorithm. Landfill area discretization with clustering block stratification is shown in Fig. 10.

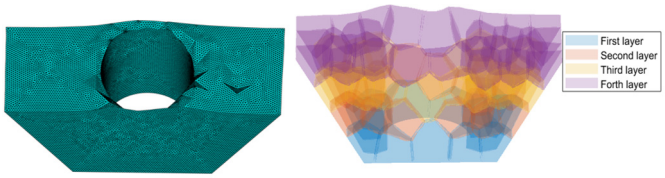

Fig. 10. Schematic diagram of discrete and layered excavation areas

The interlayer path planning is shown in Fig. 11. The complete route is shown in Fig. 12.

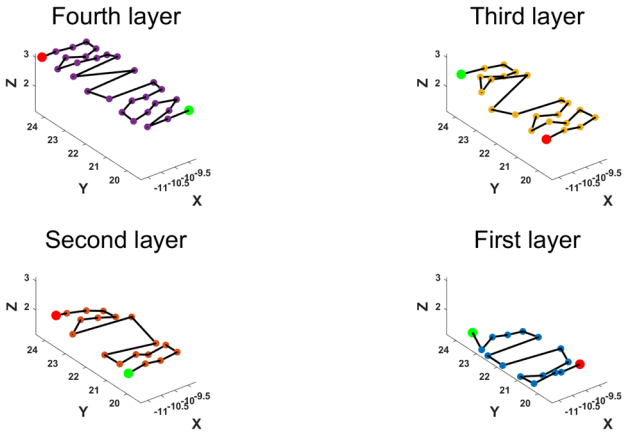

Fig. 11. Inter-layer path planning

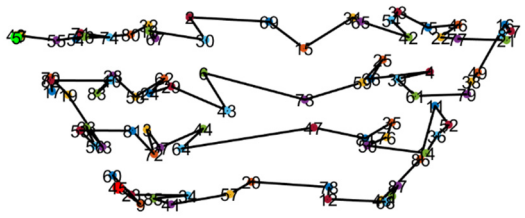

Fig. 12. Complete route

C. *Excavation and Landfill Simulation Processes*

In this study, the feasibility of a lunar soil excavation and landfill mission is verified by using a joint simulation with Gazebo[20] and ROS (Robot Operating System) platforms. Use the modeled working robot and Gazebo as a high-fidelity physical simulation environment to simulate the working process of the working robot. ROS is used as an intermediary platform to be responsible for path planning and execution of control commands. The time to excavate or landfill a piece of lunar soil is set to be 5s in the simulation, the whole excavation operation took 10 minutes and 10 seconds, and the landfill operation took 7 minutes and 15 seconds. The operation time is much smaller than the actual operation time.

After exporting the clustering blocks of excavated and backfilled areas, the effect of excavating in the order of path planning is shown in Fig. 13. The backfilling effect is shown in Fig. 14.

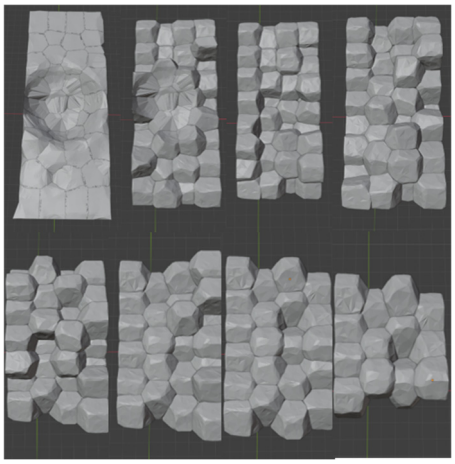

Fig. 13. Schematic diagram of the excavation process

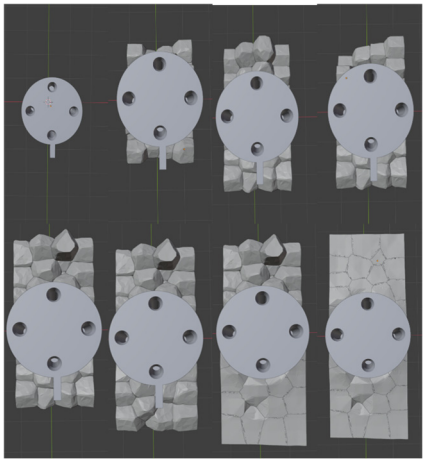

Fig. 14. Schematic diagram of the backfilling process

The excavation block model and lunar energy vehicle are imported into Gazebo. Combined with the path planning and control instructions of ROS, the simulation system can demonstrate the excavation and landfill process of lunar soil in real time, providing a basis for subsequent operation verification. The simulation process of lunar soil excavation is shown in Fig. 15.

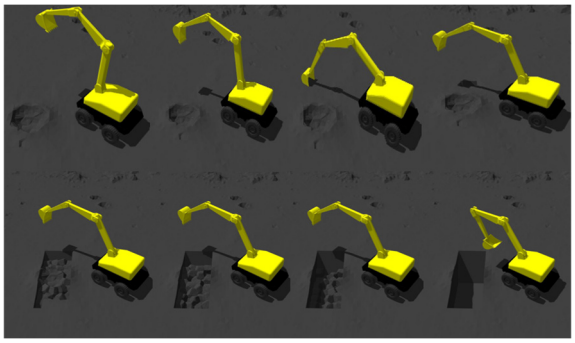

Fig. 15. Schematic diagram of excavation effect

The simulation process of lunar soil landfill is shown in Fig. 16.

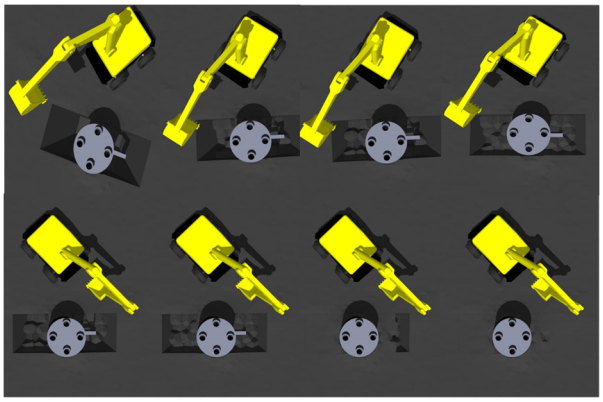

Fig. 16. Schematic diagram of landfill effect

This project proposes a method for de-discretization and geometric clustering of excavation areas based on tetrahedron geometric segmentation. It can more realistically depict the complex morphology and heterogeneous characteristics of lunar soil topography. Compared with the traditional spatial segmentation method based on cubes or regular voxels, this method shows higher geometric adaptability and simulation realism when dealing with irregular landforms and detail simplification. In addition, this method combines the three-dimensional coverage path algorithm and designs a top-down path execution mechanism for hierarchical excavation tasks. It effectively ensures the continuity and feasibility of the operation process, not only more effectively optimizes the execution order of the operation, but also reduces energy consumption.

IV. CONCLUSIONS

In this study, a simulation method of lunar soil excavation and landfill is proposed, and combined with Mini-Batch K-means clustering, Zig-zag path planning, and STL model export to successfully simulate the lunar soil excavation and landfill tasks of an operating robot during the construction of a lunar surface power station. Simulation results show that the method can realistically simulate the process of lunar soil excavation and landfill. Future work will focus on further extending the dynamics of the simulation environment and exploring more efficient data processing methods, which will provide important technical support and reference for future lunar exploration missions.

REFERENCES

[1] M.F.Palos,P.Serra,S.Fereres,K.Stephenson,and R.González-Cinca, "Lunar ISRU energy storage and electricity generation,"*Acta Astronautica*, vol.170, pp.412–420, May 2020.

[2] R.F.Garcia, "Preliminary design study for a lunar solar power station using local resources, " *Solar Energy*, vol. 86, no. 9, pp.2871–2892, Sep. 2012.

[3] S. Lumbreras and D. Pérez Grande, "Power System Concepts for a Lunar Base," *in The Human Factor in the Settlement of the Moon:An Interdisciplinary Approach*, pp.55–74, 2021.

[4] Team F S P. Fission surface power system initial concept definition. Ohio: National Aeronautics and Space Administration and Department of Energy, *NASA/TM-2010-216772*,pp.864, 2010.

[5] L. Mason, D. Poston, and L. Qualls, "System Concepts for Affordable Fission Surface Power, " *NASA/TM-2008-215166*, Jan. 2008.

[6] Kaczmarzyk M, Musiał M. Parametric study of a lunar base power systems. *Energies*, vol.14(4), pp.1141, 2021.

[7] M.A.Gibson,S.R.Oleson,D.I.Poston,and P.McClure,"NASA's Kilopower reactor development and the path to higher power missions, " in *2017 IEEE Aerospace Conference*, Big Sky, MT, USA, pp.1–14, 2017.

[8] A. Marcinkowski et al., "Lunar Surface Power Architecture Concepts," *2023 IEEE Aerospace Conference*, Big Sky, MT, USA, pp.1-19, 2023.

[9] ZHANG H,DONG K Q,YAO W.Progress and prospect of energy technologies on lunar scientific research station. *Journal of Deep Space Exploratio*n, vol.11(5),pp.423-434, 2024.

[10] I.Peake, J.La Delfa, R.Bejarano and J. O. Blech, "Simulation Components in Gazebo," *2021 22nd IEEE International Conference on Industrial Technology (ICIT)*, Valencia, Spain, pp.1169-1175, 2021.

[11] Yesmakhanova L. Modeling robotechnical mechatronic complexes in V-REP program[J]. *Informatyka, Automatyka, Pomiary w Gospodarce i Ochronie Środowiska*, vol.14, no.2, pp.141-148, 2024.

[12] Andrew Farley, Jie Wang, Joshua A. Marshall, How to pick a mobile robot simulator: A quantitative comparison of CoppeliaSim, Gazebo, MORSE and Webots with a focus on accuracy of motion, *Simulation Modelling Practice and Theory*, vol.120, 2022.

[13] M. Allan et al.,"Planetary Rover Simulation for Lunar Exploration Missions," *2019 IEEE Aerospace Conference,* Big Sky, MT, USA, pp.1-19, 2019.

[14] L. Ding, H. Gao, Z. Deng, P. Song and R. Liu, "Design of Comprehensive High-fidelity/High-speed Virtual Simulation System for Lunar Rover," *2008 IEEE Conference on Robotics, Automation and Mechatronics*, Chengdu, China, pp.1118-1123, 2008.

[15] S.C.Hicks, R.Liu, Y.Ni, E.Purdom, and D.Risso, "mbkmeans: Fast clustering for single cell data using mini-batch k-means," *PLoS computational biology*,vol.17.1, Jan.2021.

[16] X. Zhu, J. Sun, Z. He, J. Jiang and Z. Wang, "Staleness-Reduction Mini-Batch K-Means," *in IEEE Transactions on Neural Networks and Learning Systems*, vol.35, no.10, pp.14424-14436, Oct. 2024.

[17] Y. Xie, W. Hui, D. Zhou, and H. Shi, "Three-Dimensional Coverage Path Planning for Cooperative Autonomous Underwater Vehicles: A Swarm Migration Genetic Algorithm Approach",Journal of Marine Science and Engineering, vol.12(8), pp.1366, 2024.

[18] W. Qiu et al., "Terrain-Shape-Adaptive Coverage Path Planning With Traversability Analysis," *Journal of Intelligent & Robotic Systems*, vol. 110(1), pp.41, 2024.

[19] Ismail F A, Shukor S A A, Rahim N A, et al. Surface reconstruction from unstructured point cloud data for building Digital Twin. International Journal of Advanced Computer Science and Applications, vol.14(10), 2023.

[20] D. Chikurtev, "Mobile Robot Simulation and Navigation in ROS and Gazebo,"*2020 International Conference Automatics and Informatics (ICAI)*, Varna, Bulgaria, pp.1-6, 2020.